LabVIEW Simulation of Induction Motors

Zhaoxian Zhou and James Matthew Johnson
School of Computing, University of Southern Mississippi
Hattiesburg, MS 39406
Email: zhaoxian.zhou@usm.edu

Abstract - Knowledge of steady-state processes of induction motors is critical in the understanding of their operating principle. In addition to the vast, systematic theories in literature, computer simulations provide a keen insight to the mechanism. Suitable modeling methods enable motors to be simulated with various parameters. Many phenomena can be predicted without hardware experimentation. From equivalent circuits of induction motors of different power, this paper gives detailed formulations that can be used to model their steady-state performance. Simulation results are given in LabVIEW, which is a widely-adopted visual modeling platform. Various quantities such as active power, reactive power, power loss, motor slip, are demonstrated at the starting, running, and stopping of inductor motors. These visual simulations have been used by Electronics Engineering technology (EET) students for a clearer understanding of parameters that affect the operation of induction motors.

Keywords: Induction motor, Steady-state performance, LabVIEW, Simulation.

1 INTRODUCTION

Induction motors have been widely adopted electromechanical drive for industrial, commercial, and domestic applications that can operate at essential constant speed, because of their lower cost, weight and inertia, and robustness, easy maintenance, and reliability. In addition, induction machines are being used increasingly in variable-speed drives by introducing electronic power converters.

Knowledge of steady-state processes of induction motors is critical in the understanding of their operating principle. In addition to the vast, systematic theories in literature, computer simulations provide a keen insight to the mechanism. Suitable modeling methods enable motors to be simulated with various parameters. Many phenomena can be predicted without hardware experimentation. The dynamic process involves with nonlinear differential equations which are beyond the scope of most electronics engineering technology students. However the steady-state characteristics of induction motors can be easily simulated with mathematical circuit models, whose parameters can be obtained if geometric and material data of the motor are known.

Our EET program has wide coverage of LabVIEW and each student has solid skills of LabVIEW coding. In addition to hardware experiments, LabVIEW simulation is adopted for the first time in our program to study the performance of induction motors.

2 EQUIVALENT CIRCUIT OF INDUCTION MOTOR

For an efficient software simulation, equivalent circuit of induction motors must be established. The per phase equivalent circuit is plotted in Figure 1, where E_g is the source line to neutral voltage; r_1 and x_1 are stator winding resistance and leaking reactance; X_m is the magnetizing reactance; R_m is the resistance contributing to losses; r_2 and x_2 are rotor winding resistance and leaking reactance; R_x is the load resistance. For a wound-rotor motor, write $R_2 = r_2 + R_x$; for a squirrel-cage motor, $R_2 = r_2$ as there is no external

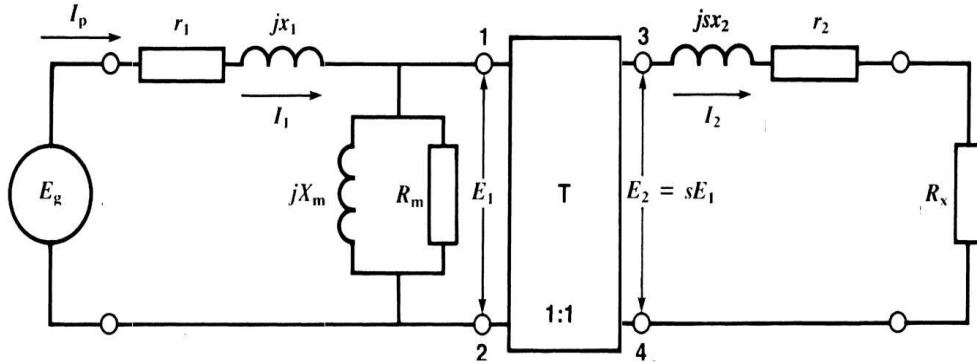resistance assumed in the simulation. s is the motor slip.

Figure 1: Equivalent circuit of induction motor

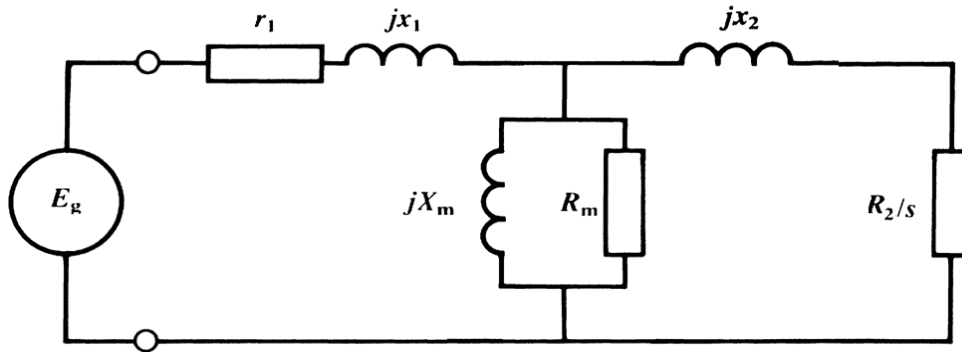At normal working condition, it is simplified to Figure 2.

Figure 2: Further Simplified Equivalent circuit of induction motor

Based on different applications, the equivalent circuits of motors can be further simplified. For small motors, the equivalent circuit is as in Figure 3 [Soe, 1]. If the power of the motor is large (for example, larger than 2 horse power), the equivalent circuit can be simplified as in Figure 4.

3 STEADY-STATE PERFORMANCE OF INDUCTION MOTOR

Base on the three equivalent circuits above, the steady-state performance can be analyzed as follows.

In general cases, the stator current is calculated by Ohm's law

$$I_s = \frac{E_g}{r_1 + jx_1 + jX_m//R_m//(jx_2 + \frac{R_2}{s})}. \tag{1}$$

Here $j = \sqrt{-1}$ and the notation $//$ is used to calculate the impedance of two parallel elements. The rotor current I_r is calculated by

$$I_r = I_s \frac{jX_m//R_m//(jx_2 + \frac{R_2}{s})}{jx_2 + \frac{R_2}{s}}. \tag{2}$$
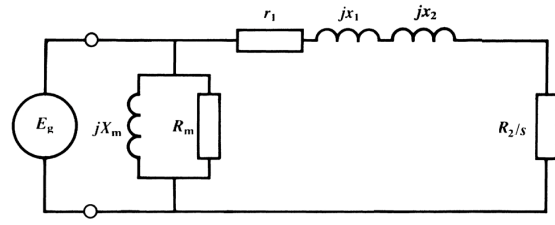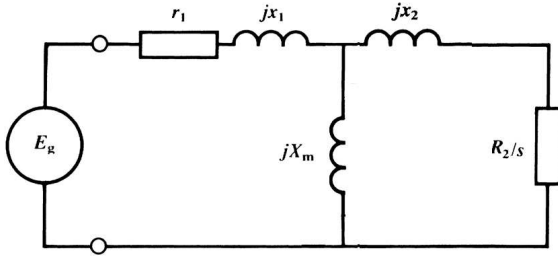
Figure 3: Equivalent circuit of small induction motor   Figure 4: Equivalent circuit of large induction motor

The complex power from the source is defined by the product of source voltage multiplied by the complex conjugate (represented by *) of the source current, *i.e.*,

$$S = E_g \times I_s^*. \tag{3}$$

the active power flow from the source is

$$P_{act} = Re(S), \tag{4}$$

and the reactive power from the source is

$$Q_{react} = Im(S). \tag{5}$$

Here Re and Im are used to represent the real and imaginary parts of the complex power, respectively.

The output mechanic power per phase is then calculated from

$$P_r = I_r \times I_r^* \frac{R_2}{s} = \frac{R_2}{s} |I_r|^2. \tag{6}$$

The corresponding torque generated by the motor per phase is

$$T = \frac{P_r}{\omega_s}, \tag{7}$$

where ω_s is the synchronous speed of the motor.

In general cases the equivalent circuit cannot be simplified. Although the calculation of quantities such as output power and mechanical torque is straightforward as stated above, the analytical formulae are lengthy because of the complexity of the circuit. However, for induction motors with very small power or with large power, the formulae are much simpler.

Following similar procedure, for small motors, the mechanical power per phase can be derived as

$$P_m = |I_r|^2 R_2 \frac{1-s}{s}; \tag{8}$$

and the motor torque per phase is

$$T_m = \frac{R_2}{s\omega_s} \frac{E_T^2}{(R_T + \frac{R_2}{s})^2 + (X_T + x_2)^2}. \tag{9}$$

2009 ASEE Southeast Section Conference

The breakdown torque is then derived as

$$T_{m_{max}} = \frac{1}{2\omega_s} \frac{E_T^2}{R_T + \sqrt{R_T^2 + (X_T + x_2)^2}}, \tag{10}$$

where E_T is the Thevenin's voltage; R_T is the Thevenin's resistance, and X_T is the Thevenin's reactance.

In fact the parameters of the equivalent circuit are not constants. They usually are functions of the stator and rotor currents. The nonlinear differential equations that can be used to describe the steady-state process are as in [Kudla, 2]. The simulation of the nonlinear equations is not covered here.

For large motors, the motor torque per phase is

$$T_m = \frac{|I_r|^2 R_2}{s\omega_s} = \frac{R_2}{s\omega_s} \frac{E_g^2}{(r_1 + \frac{R_2}{s})^2 + (x_1 + x_2)^2}. \tag{11}$$

The breakdown torque per phase is

$$T_{m_{max}} = \frac{E_g^2}{R_2 \omega_s} \frac{r_1^2 + (x_1 + x_2)^2}{4r_1^2 + (x_1 + x_2)^2}, \tag{12}$$

and it occurs when

$$s_{max} = \frac{r_1 R_2}{\sqrt{r_1^2 + (x_1 + x_2)^2}}. \tag{13}$$

4   INTEGRATING LABVIEW SIMULATIONS INTO HARDWARE EXPERIMENTS

In this section, we discuss how we integrate the software simulation of induction motors into hardware experiments. The EET program in the University of Southern Mississippi has maintained only one set of equipment for its power experiments. Due to time restriction, it is difficult for students to obtain the best experience in the induction motor experiments. The LabVIEW simulations have been implemented by our EET students and have been used by students taking *electric power generation, transmission, and distribution* class. Before entering the hardware laboratory, students conduct simulations of induction motors on the LabVIEW platform.

4.1   Impedances of the induction motor windings

The measurement of the impedances of the induction motor windings is not an objective of the simulation. Instead, the impedances should be measured in the hardware experiments. However, typical values of these impedances are given to students for simulation purpose. Students have been encouraged to verify the theoretical characteristics derived in last section with different impedances. For demonstration purpose in this paper, the input parameters for an induction motor are chosen as in [Theodore, 3]: stator resistance $r_1 = 1.5\Omega$, rotor resistance is $r_2 = 1.2\Omega$; both stator and rotor leakage reactances are $x_1 = x_2 = 3\Omega$; magnetizing reactance is $X_m = 110\Omega$; no-load losses resistance $R_m = 900\Omega$.

Based on the proposed equations, an exemplary diagram is sketched in Figure 5 and the corresponding front panel is plotted in Figure 6.
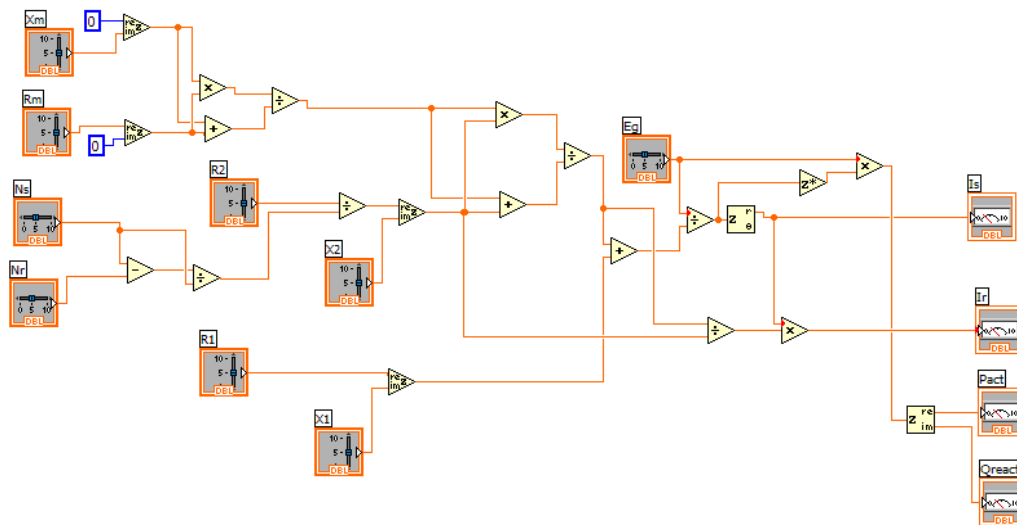
Figure 5: LabVIEW Diagram

4.2 Operating characteristics of induction motors

The starting current of an induction motor is usually greater than normal full-load current and the starting torque is thus reduced because of the reduced line voltage during start-up. The no-load current is usually less than the full-load current. Because of the large magnetizing current, the power factor of these motors is small even at full-load.

The stator and rotor current, stator and rotor power are plotted in Figures 7, 8, 9, 10.

In a non-ideal induction motor, the phase difference is much less than 90°, giving a low starting torque. Students change the input impedance by simulating a capacitor being placed in series with the starting winding, and thus improve the efficiency. The output torque and efficiency are plotted in Figures 11, and 12.

In the following hardware laboratory, students are required to set up and conduct several motor experiments:

- to measure the resistance of windings of a split-phase motor;

- to measure the starting and operating characteristics of the split-phase motor under load and no-load conditions;

- to study the power factor and efficiency of the split-phase motor;

- to measure the starting and operating characteristics of the capacitor start motor.

Similar to what is performed in the software laboratory, students take measurements required to compute motor parameters and examine the motor characteristics under varying working conditions. Feedbacks from the hardware laboratory section show that due to the experience gained during the software laboratory, students appear to be more familiar with the theory and operation of induction motors.
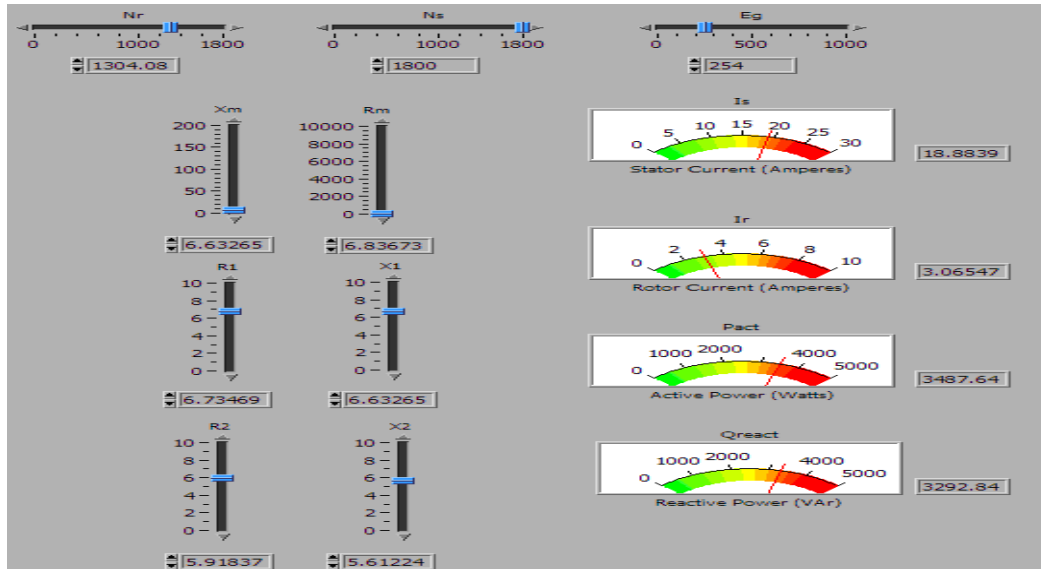
Figure 6: LabVIEW VI front panel

5 CONCLUSION AND FUTURE WORK

In this paper, different equivalent circuits of induction motors are discussed. Formulations are proposed to calculate stator and rotor currents, various powers from the source. Constant circuit parameters in steady-state operations are assumed. These formulae have been used to guide the LabVIEW modeling by students. The adoption of the software simulation among EET students before their hardware experiments gives them a better understanding of operating principle of induction motors. There are two tasks to be investigated in the future: steady-state performance with nonlinear parameters and dynamic performance of three-phase induction motors. These simulations will be available for use in the next academic year.

6 REFERENCES

[1] N. N. Soe, T. T. H. Yee, and S. S. Aung, "Dynamic modeling and simulation of three-phase small power induction motor," in Proceedings of World Academy of Science, Engineering and Technology, vol. 32, August 2008, pp. 451454.

[2] J. Kudla, "Use of induction motor steady-state characteristics determined by means of the finite element method for parameter estimation of motor nonlinear circuit model," in Proceedings of the 11th International Symposium on Applied Electromagnetics & Mechanics, Versailles, France, May 12-14 2003.

[3] Theodore, Electrical Machines, Drives, and Power System, 6th ed. Upper Saddle River, NJ: Prentice Hall, 2006.

Biography

Zhaoxian Zhou received the B. Eng. from the University of Science and Technology of China in 1991; M. Eng. from the National University of Singapore in 1999 and the PhD degree from the University of
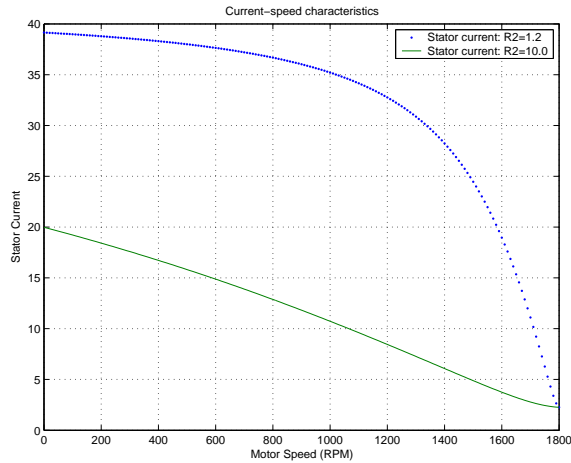
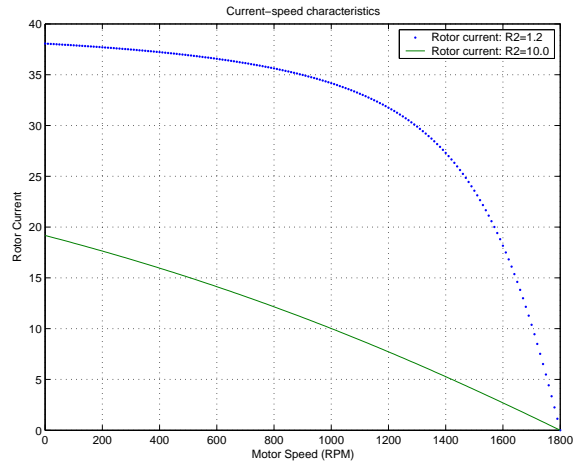Figure 7: Stator current speed characteristics

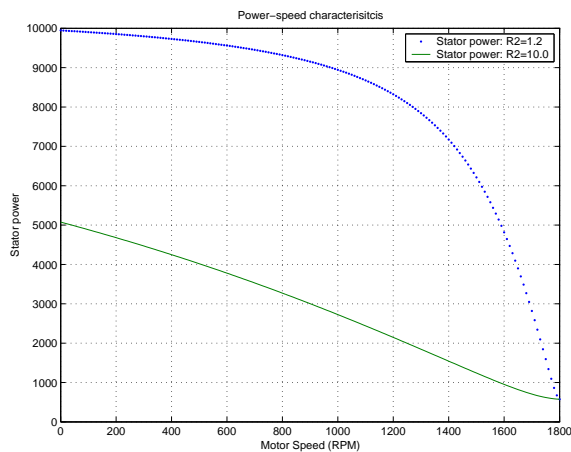Figure 8: Rotor current speed characteristics

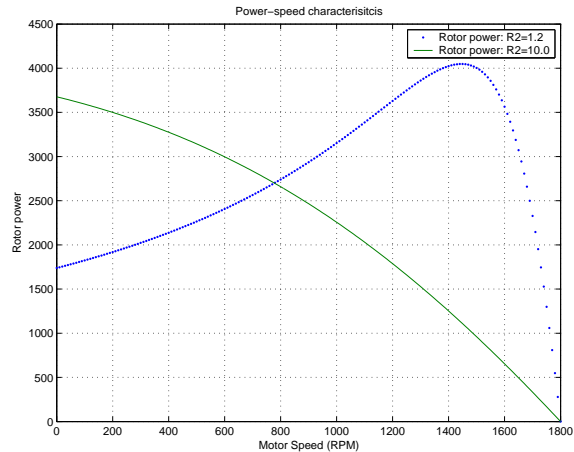Figure 9: Stator power speed characteristics

Figure 10: Rotor power speed characteristics

New Mexico in 2005. All degrees are in Electrical Engineering. From 1991 to 1997, he was an Electrical Engineer in China Research Institute of Radiowave Propagation. In the fall of 2005, he joined the School of Computing, the University of Southern Mississippi as an assistant professor. His research interests include electromagnetics, radiowave propagation, high performance computing and numerical analysis. His teaching interests include communications, electromagnetics, antennas and propagation, electric power, and signal processing. He is a senior member of IEEE and a member of ASEE.

James Johnson is from Terry, Mississippi, and holds an Associate of Arts Degree in Pre-Engineering from Hinds Community College in Raymond, Mississippi. He is currently a senior at the University of Southern Mississippi, majoring in Electronics Engineering Technology with a minor in Computer Engineering Technology. His interests include communications, computer networking, digital logic, and programmable logic controllers. He is a student member of IEEE and ISA.
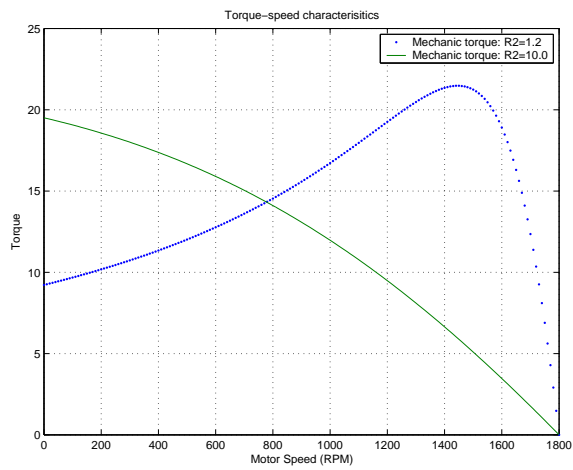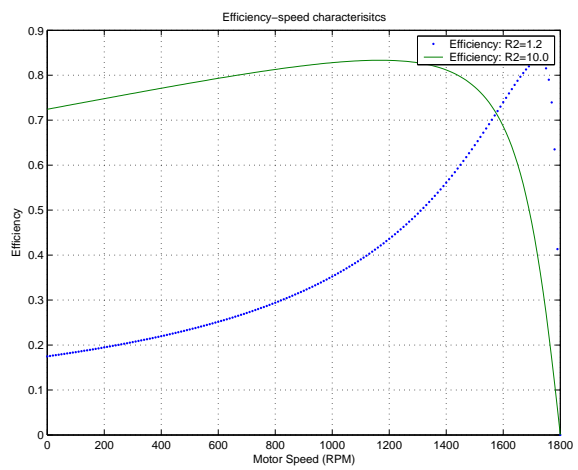
Figure 11: Torque speed characteristics

Figure 12: Efficiency speed characteristics